Chapter 8

From Color-Matching Error to Large Color Differences

Color differences have been scaled from the level of color-matching error, through threshold and industrially important suprathreshold small color differences, large differences of the size in OSA-UCS, all the way to quadrant-sized differences. In all cases considered here the difference judgments have been made against a simple achromatic surround. In previous chapters we have seen that there are systematic changes in terms of stimulus increments, depending on the magnitude of the difference. In this chapter color differences of varying sizes are compared in terms of stimulus increments to assess commonalities and divergences.

8.1 A COMMON BASIS FOR COMPARISON

It is of interest to compare such data both in L, M, S cone sensitivity space as well as the CIE tristimulus space. Aside from scale differences the main difference between the two is that in case of the former comparison is made at the point of interaction of light energy with cones, while in the latter case it is made in a system that implicitly accounts for the reappearance of red at the shortwave end of the spectrum and recognizes luminance and chromaticness as important color attributes. Conversion to the L, M, S space has been cal-

Color Space and Its Divisions: Color Order from Antiquity to the Present, by Rolf G. Kuehni
ISBN 0-471-32670-4

culated using the Smith-Pokorny definition of cone sensitivities. All comparisons are made assuming an equal energy light source.

Historical color-matching error (CME) and suprathreshold small color difference data have usually been expressed in form of ellipses or ellipsoids in the CIE chromaticity diagram or the x, y, Y space. More recently they typically have been expressed in the L^*, a^*, b^* space or a cone contrast diagram. Systematic studies of threshold differences and color-matching error have started with the work of Wright (1941) and MacAdam (1942). MacAdam continued the CME work together with Brown (1949), followed by Brown's work (1957) with twelve observers. Additional CME data were contributed by Wyszecki and Fielder (1971a). These authors also reported on a different kind of experiment where a chromatic difference was displayed and the observer had to select a third color so that the chromatic differences between the three colors were equally large (1971b). The variability in the setting of the third color was then determined (CDM data). Richter reported in 1985 on an extensive determination of threshold data. For the purposes of comparative analysis it has been assumed that CME data represent object colors at a luminous reflectance of $Y = 30$.

As mentioned earlier, a collection of suprathreshold small color difference data based on several experiments using object color samples was assembled, in parts modified, and normalized by Luo and Rigg in 1986 (L-R data). A portion of these data, limited in luminous reflectance to the range $Y = 25$–35, have been used in this analysis. Other sets of suprathreshold small color difference data, such as the RIT-DuPont (R-D) data, were not considered here because their range of luminous reflectance values is large, with a small amount of data near $Y = 30$. Some of the data, including the R-D data, were used to compare lightness scaling. There are several sets of published large color difference data: Munsell, OSA-UCS, data by Wyszecki and Wright (1965) developed in connection with a field trial for a color difference formula, and the more recent Guan and Luo (1999) data. Color difference formulas as representative approximate models of small and large color difference experiments, CIELAB and CIE 94, have been used for comparison purposes.

Observer groups for the various experiments were obviously different, and there were also many differences in observing conditions. Inconsistencies between different data sets of the same type presumably are due to different observer groups and/or different observation/test conditions. They also may be due to effects so far not considered. Among these may be, as mentioned earlier, the issue of significant variation in the apparent composition of the lightness signal as well as the difference in sensitivity of yellow-blue and green-red opponent systems found for different observers, the uncertainty of constant chroma contours and constant hue differences (and very likely individual variations thereof), and the resulting partial conflation of lightness, chroma, and hue differences.

8.2 CHROMATIC AND LIGHTNESS CRISPENING EFFECTS

In 1949 Le Grand analyzed the MacAdam ellipses in terms of increments in two slightly different sets of three color fundamentals, R, G, and B. His results indicated that for either set the experimental ellipses, when projected onto the R, B plane, were nearly aligned with the axes of that plane, with the longer semi axis aligned with the B axis and the shorter one with the R axis. When plotting the increments representing the semi axis length as a function of the value of the fundamental he found a function (similar to Fig. 8-1*a*) linear over a large portion for B increments and a V-shaped one (similar to Fig. 8-1*b*) for R increments. Boynton and Kambe reported comparable results in 1980 from investigation of the size of incremental thresholds along lines of constant values of fundamentals (note that these were not CME data). The increments in B could be modeled as a constant fraction of B over a large range. Increments in R also confirmed the V-shape centered on the achromatic point, discovered by LeGrand. Nagy et al. (1987) investigated CME data (MacAdam, Brown-MacAdam, and Wyszecki-Fielder) and essentially confirmed the Boynton and Kambe (and thereby the Le Grand) results. They fitted a Fechnerian formula to the ΔS versus S function and a more complex formula relating L and M and containing a component of S to the ΔL versus L function. The authors explained the V-shape of the latter function as "opponent interactions between the two long-wavelengths cone mechanisms." As an

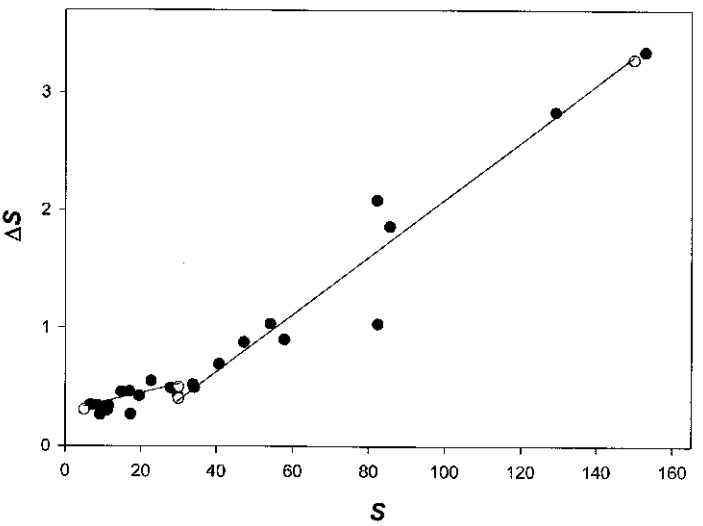

Fig. 8-1a *Increments in* S *as a function of* S *for the MacAdam ellipses (excluding ellipse 1). Open circles represent points calculated by linear regression. They are connected by linear regression lines.*

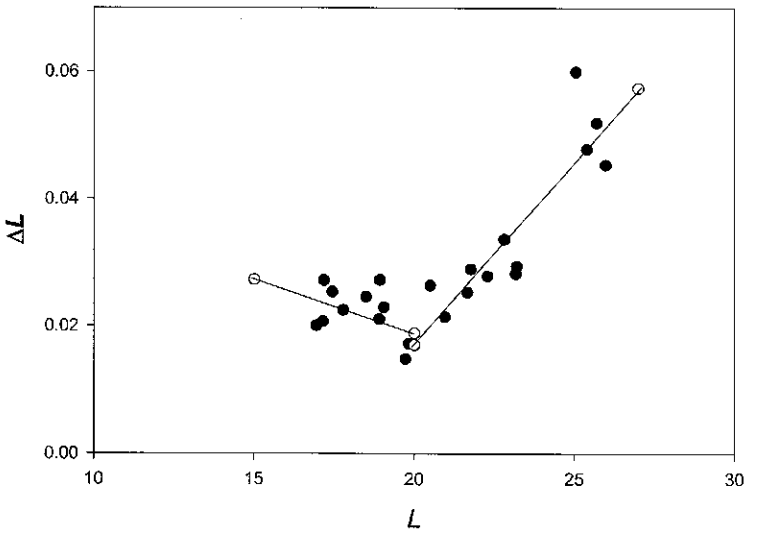

Fig. 8-1b *Increments in* L *as a function of* L *for the MacAdam ellipses (excluding ellipse 1). Open circles represent points calculated by linear regression. They are connected by linear regression lines.*

aside, in a previous investigation Boynton et al. (1983) found that individual observers differ in the relative sensitivity of their two opponent color systems by more than a factor of 3.

Schönfelder, Kaneko, Takasaki, and others, as discussed in Chapter 4, have found that threshold or unit larger difference increments determined against an achromatic surround require the smallest stimulus increments/decrements at the surround chromaticity. The required stimulus changes increase in magnitude as the distance from the achromatic point increases. In case of lightness differences the smallest change is also required at the lightness of the surround.

Tristimulus values for the equal energy illuminant representing CME and color difference data have been converted to Smith-Pokorny cone sensitivity data and plotted as ΔS against S and ΔL against L (Kuehni, 2001d), and linear models were fitted separately to both sides of the achromatic point. As mentioned, in the case of CME data, determined in visual colorimeters, the simplifying assumption was made that they are object colors with a luminous reflectance of $Y = 30$. In case of the Brown-MacAdam and Brown data with variable luminosity, this was considered justified by MacAdam's finding that the size of CME ellipses varies by less than 20% as a function of luminosity in a medium range of luminosities. Figures 8-1*a* and *b* illustrate the increment functions for the MacAdam ellipses (minus ellipse 1).[1] There is a fair amount of variation and the regression lines do not intersect exactly at the achromatic point. It is evident that both cases can be seen as representing V functions with different angles of opening of V. Such a situation is what one would expect

from the functioning of the chromatic crispening effect. Increments are, in terms of stimulus, smallest at the surround chromaticity (achromatic point) and grow, absolutely or at least relatively, in both directions away from that point. The magnitude of the effect is different for L and S, in part due to the fact that colors of constant luminous reflectance can differ much more in S than in L or M, as we have seen earlier. (Because of the large degree of overlap with L, the function for M is very similar to that of L and not shown.)

Comparable results have been obtained for all CME and suprathreshold small color difference data. All slopes for L of colors where L is smaller than that of the achromatic color are negative. In case of S it is negative for observer GW in the Wyszecki-Fielder data. It is much less positive in all other cases than that of the increments for colors with S larger than that of the neutral point (except for the Brown-MacAdam data [observer WRJB] where there is no apparent chromatic crispening effect involving S). A negative slope for S less than that of the achromatic point is implied in the CIE 94 color difference formula. Figure 8-2*a* and *b* illustrates the two functions calculated from a series of CIE 94 ellipses in the a^*, b^* diagram with a constant total color difference.

The results indicate that the chromatic crispening effect is active, as one might expect, in every set of CME, threshold and suprathreshold small color difference data investigated. Its activity is implied in the S_C function of the CIE 94 formula and comparable functions in other color difference formulas. The angle of opening of the V-shaped functions ΔL versus L and ΔS versus S for various sets of data are given in Table 8-1. The angles are only comparable within one type of function (the Richter data are not directly comparable because the average Y is 16.5, rather than 30 as in all other data sets).

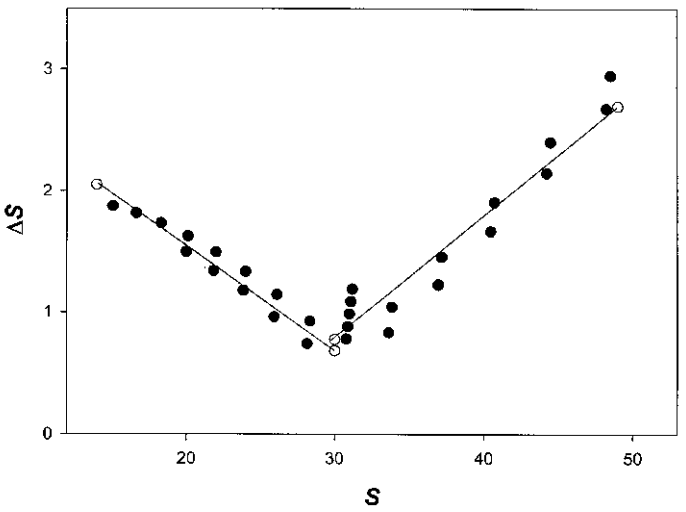

Fig. 8-2a *Increments in* S *as a function of* S *for a series of ellipses according to the CIE94 formula in the* a*, b* *diagram.*

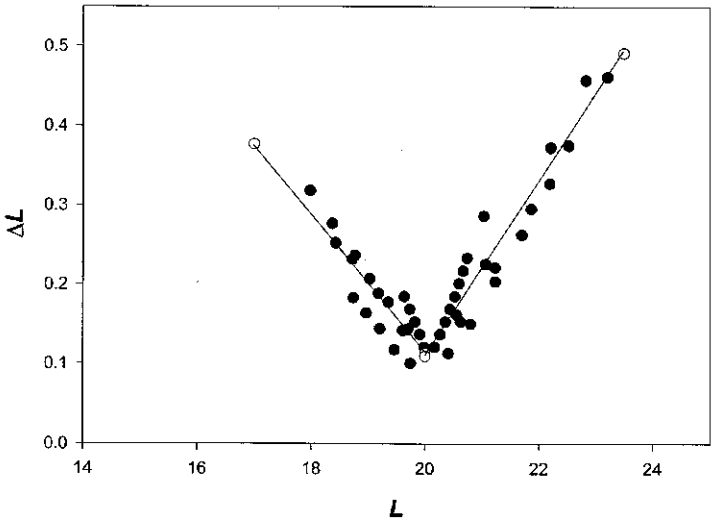

Fig. 8-2b *Increments in* L *as a function of* L *for a series of ellipses according to the CIE94 formula in the* a*, b* *diagram.*

TABLE 8-1 Comparison of angles of opening of the V-shaped functions of ΔL versus L and ΔS versus S in various data sets

Data set	Angle, deg *L* Function	Angle, deg *S* Function
MacAdam	110	142
Brown-MacAdam (observer WRJB)	147	180
Brown (weighted averages)	126	124
Wyszecki-Fielder CME (observer AR)	74	149
Wyszecki-Fielder CDM (observer GW)	81	141
Luo-Rigg ellipses (Y = 25–35 only)	110	116
Richter (Y = 16.5)	144	144
CIE 94	73	106

The results show that the V functions implied in CIE 94 are more sharply angled than those of all experimental data sets. This indicates that the S_C function of that formula adjusts for more than the chromatic crispening effect. The implication is that unit small color difference contours in the a^*, b^* diagram adjusted for chromatic crispening are oval in form. The additional effect of S_C is to convert the elongated contours to circles of equal size, as will be seen later.

Using ellipses in the a^*, b^* diagram fitted to the Luo and Rigg and the RIT-DuPont (R-D) data (Melgosa et al., 1994, 1997), one can determine the average change in chromatic ellipse size at an approximately constant luminous reflectance. The average axis length (between $L^* = 56$ and 64, $n = 30$) increases by a factor 4.4 from chroma 0 to chroma 100 as a result of the chromatic crispening effect.

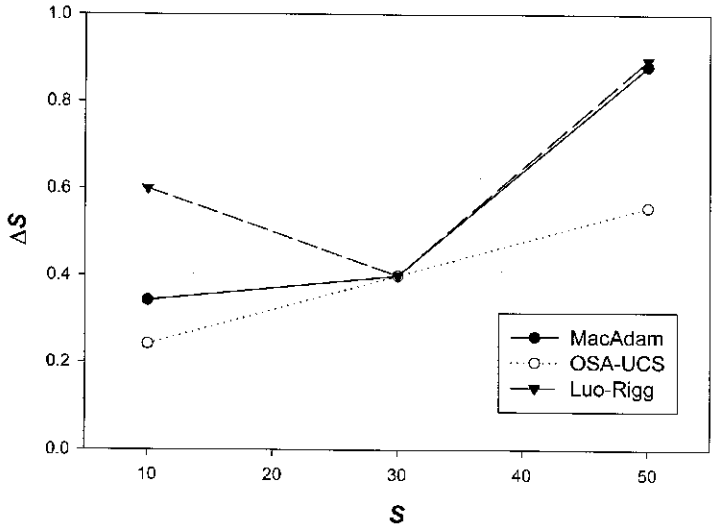

Fig. 8-3a *Regression lines of* ΔS *versus* S *of the selected Luo-Rigg (*Y *= 25–35) and OSA-UCS data normalized at the neutral point to those of the MacAdam data.*

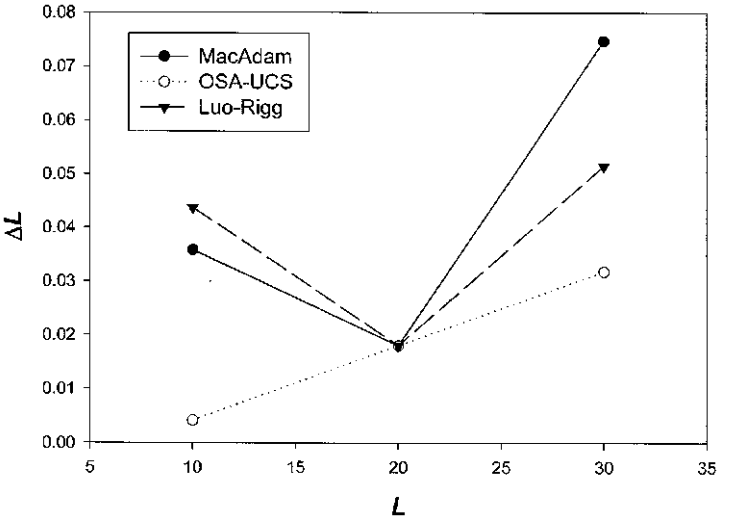

Fig. 8-3b *Regression lines of* ΔL *versus* L *of the selected Luo-Rigg and OSA-UCS data normalized at the neutral point to those of the MacAdam data.*

In Fig. 8-3*a* and *b* the regression lines of the ΔL versus L and the ΔS versus S functions of the L-R and the OSA-UCS data sets have been normalized at the neutral point to those of the MacAdam data. Interestingly, for both cone types the L increments are larger for colors both greenish and yellowish for

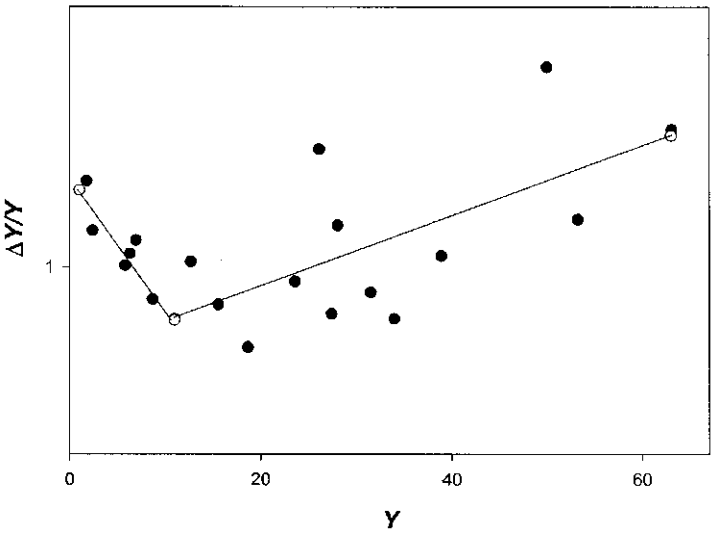

Fig. 8-4 *ΔY/Y as a function of* Y *for the RIT-DuPont data. Open circles represent points calculated by linear regression. They are connected by linear regression lines. Surround luminous reflectance* Y = *11.*

the L-R data compared to the MacAdam data, and vice versa for the colors both reddish and bluish.

A generally comparable situation applies to lightness crispening. We have seen in Chapters 5 and 7 that lightness crispening is implicit in all experimentally determined lightness scales. When plotting ΔL versus L of the luminous reflectance scale (or ΔY versus Y) we can expect to find a similar V shaped form as in the case of chroma crispening, if the surround luminous reflectance falls between the extremes of that of the test colors. Since in all CME data the surround luminosity was lower than that of the least luminous test field a V-shaped function is not expected in the data with variable luminosity, as indeed is not the case. In the R-D data, where the surround luminous reflectance was $Y = 11$, the effect is present but small, best illustrated by plotting the Weber fraction of Y versus Y (Fig. 8-4). In terms of ΔL versus L we can find the effect when plotting this function for OSA-UCS lightness that has lightness crispening for $Y = 30$ built into the formula. The crispening effects indicate that the Weber-Fechner law is not applicable to color differences throughout the range of size where the crispening effects are applicable.

8.3 CHROMATIC CRISPENING FADES AS A FUNCTION OF THE SIZE OF THE DIFFERENCE

When plotting ΔL versus L and ΔS versus S for colors of the Munsell and the OSA-UCS systems along the axes in the a^*, b^* diagram, we find no chroma crispening effect, and there is a continuous increase with a positive slope.

The same applies for constant size chroma differences as calculated by the CIELAB formula. When optimizing the divisor in S_C for these color series, it is found to be near 1 (Kuehni, 2001c). It is 1 when optimizing it to the hue and chroma difference optimized OSA-UCS formula for the basis data of that set (see Chapter 7). Guan and Luo (1999) optimized a modified CIE94 formula to various sets of large color difference data, and found different optimal S_C and S_H factors. They recommended for large differences a formula in which the S_C divisor is $1 + 0.016C^*$ and the S_H divisor is 1 (compared to S_C divisor $1 + 0.045C^*$ and S_H divisor $1 + 0.015C^*$ in CIE 94, GLAB, see chapter 6). An explanation for these findings is that chromatic crispening fades as the size of the chromatic difference increases. This is surprising and different from lightness where lightness crispening is present from color-matching error to large differences.

In the absence of detailed experimental data one can estimate the relative magnitude of the adjustment for the chromatic crispening effect in small color difference perceptual data and the effect of converting ellipses to circles in the S_C divisor. If we assume the length of the major axis at the neutral point to be 1.5 (the average of 7 ellipses with $C^* < 2$ is 1.55) and the increase in axis length as a function of the chromatic crispening effect (see above) a factor 4.4, the total value of the S_C divisor should be 6.6 at metric chroma 100. It is found to be only 5.5 in CIE94, a reasonable result given the variability in the visual data.

It seems likely that this change in implied S_C is located on a continuous function, as estimated in Fig. 8-5. Systematic experiments are required to clarify the shape of the function.

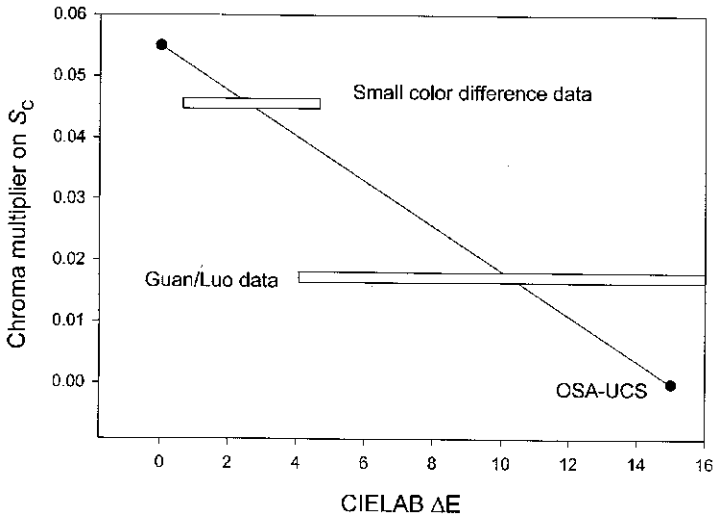

Fig. 8-5 *Chromatic chrispening as represented by optimized* S_C *divisor as a function of size of CIELAB* ΔE *differences for three sets of data and linear estimate of the function relating the two. The boxes represent the approximate ranges of differences in the data sets.*

8.4 SIZE AND RATIO OF UNIT INCREMENTS

Calculation of the linear regression lines of incremental data allows comparison of the size of the unit increments. Because of the different magnitude of the chromatic crispening effect in different data sets meaningful comparison is only possible of the implied first step from the achromatic point. These are compared in Table 8-2 in the direction of higher L respectively S values.

Several observations and conclusions can be drawn from the data in this table:

1. MacAdam and Brown-MacAdam data are very similar.
2. Observers GW and AR differ significantly in their sensitivity to sub threshold L differences.
3. The Brown average data differ significantly, either as a result of the weighted averaging process or for other reasons, from the other CME data.
4. The color difference matching error is elevated by approximately a factor 2 from the color-matching error.
5. The Richter threshold data indicate a higher L increment compared to CME data but a lower S increment, resulting in a significantly lower ratio.
6. The selected L-R data also have a lower ratio and even more pronouncedly the CIE94 and the CIELAB formulas.

TABLE 8-2 Comparison of unit *L* and *S* increments for the first step from the neutral color toward higher *L* and *S* values and their ratio for various data sets based on linear regressions, *Y* = 30

Data set	*L* Increment	*S* Increment	Ratio
CME data			
MacAdam	0.0168	0.40	23.8
Brown-MacAdam	0.0232	0.60	25.8
Wyszecki-Fielder/GW	0.0191	0.72	37.9
Wyszecki-Fielder/AR	0.0300	0.78	26.0
Brown	0.0410	0.21	5.1
Wyszecki-Fielder/CDM	0.076	1.53	19.7
Threshold and small color difference data			
Richter (extrapolated to $Y = 30$)	0.036	0.38	10.6
Luo-Rigg data	0.045	0.63	14.0
Large difference data			
Munsell	0.373	6.00	16.1
OSA-UCS	0.529	8.22	15.5
Color difference formulas			
CIE94/DE = 1.0	0.043	0.31	7.2
CIELAB/DE = 1.0	0.103	0.66	6.4

TABLE 8-3 Comparison of unit increment values of *X* and *Z* for the first step from neutral for selected data, based on regression calculation at *Y* = 30

Data set	*X* Increment	*Z* Increment	Ratio
CME data average (excluding Brown)	0.136	0.625	4.6
Luo and Rigg	0.279	0.629	2.3
Color difference matching data	0.471	1.50	3.2
Munsell data	2.35	6.03	2.5
OSA-UCS	3.23	8.22	2.5
CIELAB formula, DE = 1.0	0.639	0.658	1.0
CIE94 formula, DE = 1.0	0.265	0.310	1.2

7. Munsell and OSA-UCS have similar ratios, and the OSA-UCS steps are approximately 1.4 times larger than two Munsell chroma steps, as we have seen in Chapter 7.

The average L increment of the CME data (excluding the Brown data) is 0.022, the S increment 0.625, for a ratio of 28.4. For the L-R data selection, the ratio is 14.8. It is evident that a significant change is happening between imperceptible color-matching errors and small color differences: while S increments are nearly the same it is L increments that become larger in small color differences by approximately a factor of 2. The ratio remains essentially the same when the differences are large. The color difference matching error has a ratio smaller than that of color-matching error but larger than that of color differences. The Richter threshold data with a ratio of 10.6 are an exception to the picture, due to a very low S increment.

When data are viewed, in the CIE tristimulus system a more familiar picture emerges. Table 8-3 contains a selection of the data of Table 8-2 expressed in terms of X and Z (the latter identical to S).

Small and large color difference data have comparable ratios of approximately 2.5. The CIELAB formula, by definition, has a ratio of 1, due to the factor of 2.5 between the multipliers of a^* and b^* (500/200). CIE94, due to the effect of S_C, has a slightly larger ratio. Unsurprisingly, the key difference remains the same: while in the CME and small color difference data the Z increments are the same, the X increment increases by an approximate factor of 2 in the small and large color difference data, compared to CME data. It should be recalled that the multiplier balancing the linear opponent color functions a and b is 2.3 to 2.4, depending on the standard observer. The implication is that color difference perception regards the balanced a and b systems as equivalent.

On the other hand, color-matching errors appear based only on the sensitivity limits of the cones. (Here the findings of Boynton and Kambe, 1980, of thresholds along constant S and constant $L/2M$ lines are not in agreement, since they largely duplicated, if with larger Weber fractions, MacAdam's results.) Color-matching error data and color difference data are, it appears,

incommensurable, and geodesics based on color-matching error data do not predict geodesics of color difference data. The Richter threshold data, as one would expect, fit into this picture as indicated by an, albeit low, ratio of 1.7.

8.5 DIRECTION OF UNIT CHROMATIC CONTOURS IN THE *L, M, S* AND *X, Y, Z* SPACES

The difference between CME and color difference data is further clarified when comparing the shape of their chromatic contours in L, M, S and X, Y, Z spaces. For this purpose the intersection points of the major and minor axes of the unit contours are translated into these spaces and views in certain directions are created. The exercise is limited to representative data: the MacAdam ellipses and the Wyszecki-Fielder (observer GW) data as representative for CME data and the Luo-Rigg data for small suprathreshold color differences. Figures 8-6 to 8-8 illustrate the ellipses, each represented by five points (the endpoints of the long and short ellipse axes in the a^*, b^* diagram and the centerpoint), for the three cases in the L, S view. A number of observations

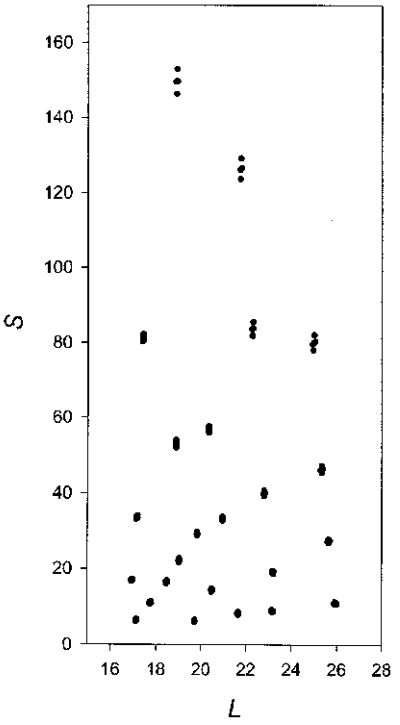

Fig. 8-6 *MacAdam ellipses represented by the center point and the four points of the ellipse intersections with the major and minor axes, in the* L, S *cone response diagram, equal energy illuminant.*

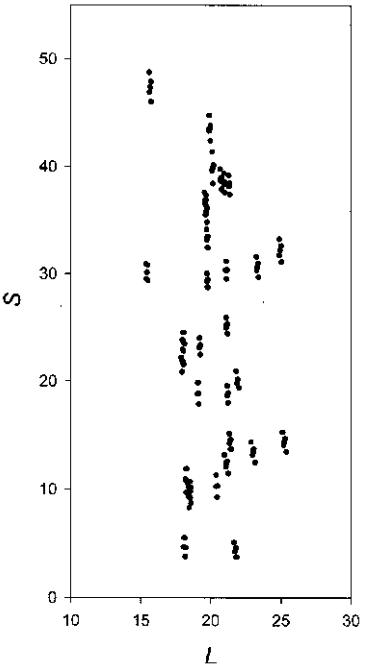

Fig. 8-7 *Selected Luo-Rigg ellipses represented by the center point and the four points of the ellipse intersections with the major and minor axes, in the L, S cone response diagram, equal energy illuminant.*

TABLE 8-4 Angles of major ellipse axis against abscissa in the *L*, *S* and *X*, *Z* diagrams

Data set	Number of Angles		Mean Angle, deg	Range, deg	COV, %
	<90	>90			
L, S diagram					
MacAdam	16	9	89.8	86.2–96.0	0.1
Wyszecki-Fielder/GW	5	23	92.6	87.0–101.0	3.9
Wyszecki-Fielder/AR	8	20	91.0	87.9–99.9	2.1
Luo-Rigg (Y = 25–35)	5	26	93.1	86.1–99.4	3.5
X, Z diagram					
MacAdam	22	3	77.4	57.4–115.0	16.8
Wyszecki-Fielder/AR	21	7	87.9	65.1–136.5	19.8
Luo-Rigg	9	22	96.8	56.9–130.6	19.2

can be made from the results. The MacAdam ellipses are well aligned with the axes of the diagram; that is, they are well described by differences in L and S. Table 8-4 contains data concerning the angles against the abscissa of the major ellipse axis for some data sets in both the L, S and the X, Z diagrams.

The essentially vertical alignment of the MacAdam ellipses in the L, S

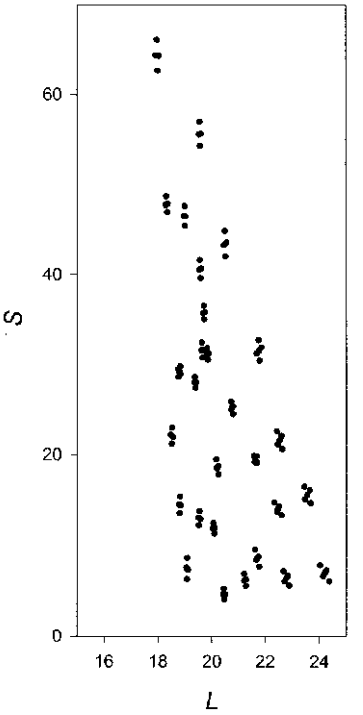

Fig. 8-8 *Wyszecki-Fielder (observer GW) ellipses represented by the center point and the four points of the ellipse intersections with the major and minor axes, in the* L, S *cone response diagram, equal energy illuminant.*

diagram is confirmed by the statistics. Both Wyszecki-Fielder observers show a bias toward angles larger than 90°, primarily due to a counterclockwise rotation of contours in quadrant 4 (yellowish-reddish colors; Fig. 8-8). This effect is stronger in the GW data. The bias in the L-R data is comparable to that of observer GW.

Because of the rotation in space and the rescaling of the X compared to the L axis, the picture looks different in the X, Z diagram, as shown in Figs. 8-9 and 8-10. Here most MacAdam ellipses have a strong bias toward a smaller angle, and the variability in angles has increased significantly. The AR data have a similar tendency and the variability in angles is even larger. The L-R data continue to have a bias toward angles larger than 90°, also with a high variability. Here the tendency of many ellipses is to point in the direction of the neutral point (at $X, Z = 30$). The X, Z diagram is a not a normalized version of an opponent color diagram, and in a normalized diagram the tendency is even clearer. The implication is that these ellipses are aligned along constant hue lines and represent the larger increment required for a unit chroma difference compared to a unit hue difference of the same perceptual size. This tendency is also apparent in one quadrant for observer GW, less so for observer AR. In

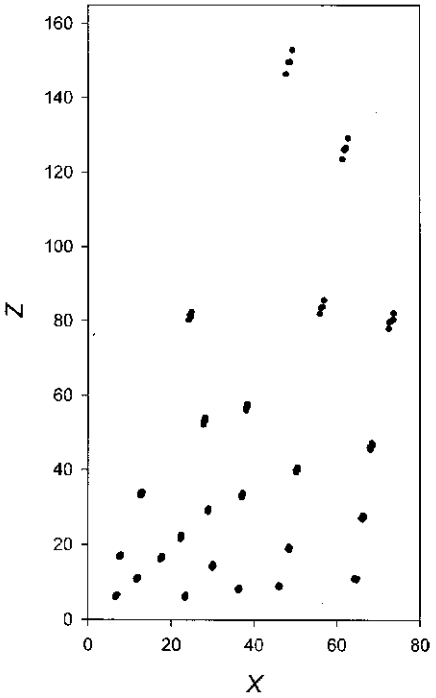

Fig. 8-9 *MacAdam ellipses represented by the center point and the four points of the ellipse intersections with the major and minor axes, in the* X, Z *diagram, equal energy illuminant.*

the Munsell system the contours, as we have seen in Chapter 7, are uniformly aligned along radial lines. In the X, Z diagram this is more or less the same.

The conclusions one can draw is that under the conditions of the MacAdam experiment and/or as a result of the vision properties of that observer the color-matching error is caused by limitations in cone sensitivity only. In the conditions of the Wyszecki-Fielder experiment yellowish-reddish colors of quadrant 4 point toward the neutral point, but the ratio between the two axes remains average for CME data. An opponent color system appears active in case of the L-R suprathreshold data. Here in addition the L, respectively X, unit increment is increased compared to the S or Z increment in accordance with global requirements for uniformity.

8.6 THE PARADOX OF HUE DIFFERENCES

Pages of the Munsell or NCS atlases contain by design colors of constant hue at different levels of lightness and chromaticness. One might assume that the hue differences between corresponding colors on two adjacent pages are all of identical size, since they all bear the same respective hue names (i.e., that hue

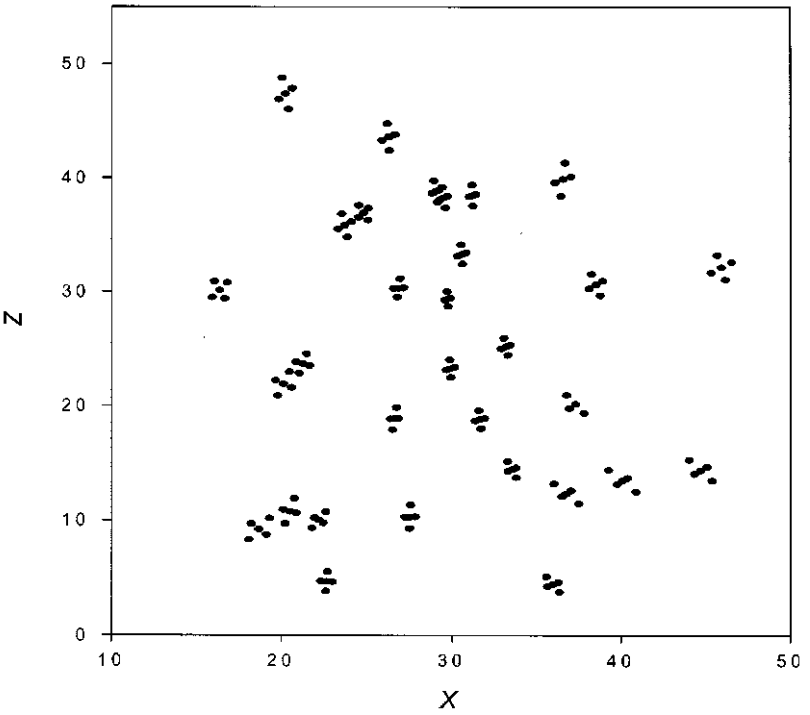

Fig. 8-10 *Selected Luo-Rigg ellipses represented by the center point and the four points of the ellipse intersections with the major and minor axes, in the* X, Z *diagram, equal energy illuminant.*

differences are independent of chroma and lightness differences). Diagrams such as the Munsell psychological chromatic diagram or the CIELAB diagram show a much different picture. The CIELAB formula predicts that the hue difference between two colors of identical chroma and lightness, and differing only in hue, varies by a factor of 10 between metric chroma of 10 and 100. A comparable result is implicit in the Nickerson Index of Fading. The paradox is that two pairs of colors with the same hue names at two different chroma levels with the same hue angle difference have a calculated Nickerson or CIELAB hue difference differing by a factor of 10. (It should be noted that in the CIELAB formula hue superimportance is not considered and the ratio between unit hue and chroma difference does not conform to the visual ratio.) If this is valid, the implication is that at metric chroma 100 there should be 10 times more distinguishable hue differences compared to metric chroma 10. Hue, of course, fades at the achromatic point and hue differences disappear also. The author is not aware of any study other than Nickerson's where the size of perceived hue differences between sets of Munsell colors of constant hue as a function of chroma and lightness was investigated explicitly. The Munsell BOC illustrates all forty hues down to chroma 2 and half of them to

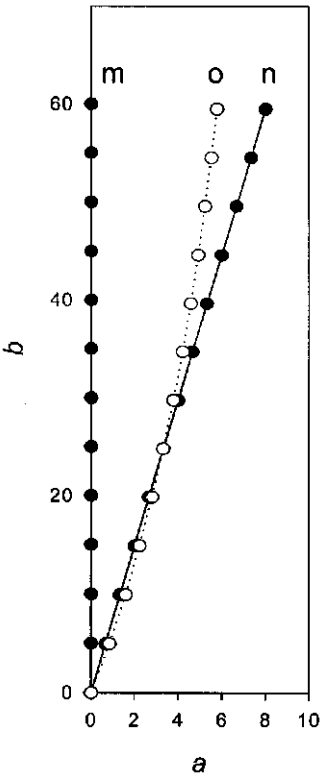

Fig. 8-11 *Lines connecting two hypothetical series (*m *and* n*) of colors of constant hue in a perfect hue circle. Line* o *represents the colors of line* n *after application of the* S_H *hue difference weight in the CIE94 color difference formula, normalized at metric chroma 25.*

chroma 1. The only (implied) quantitative psychophysical data we have in this matter are those used to determine the S_H factor in the CIE94 and similar formulas. It should be recalled that it is based on fitting a formula to elliptical contours in the a^*, b^* diagram so that they become circles of equal size. No hue difference judgments have been made in its support.

When plotting the hue differences implicit in CIE94 and similar formulas as a function of metric chroma (Fig. 8-11) we find a different picture applicable at the small color difference level. Figure 8-11 schematically illustrated two series of colors each of constant hue but varying in chroma. The hue angle between members of the two series is constant. Line *o* shows the effect of the S_H factor, normalized at $C^* = 25$. The result is in better agreement with informal evaluations of the Munsell hue circle: perceived hue difference between constant hue pairs fades to zero at the achromatic point but more gradually than the CIELAB formula implies. If the hue difference between line *m* and the normalizing point on line *o* is 1.0, it is 1.4 at chroma 10 and 0.30 at chroma 100. That is to say, colors on neighboring equal hue lines differ nonlinearly in

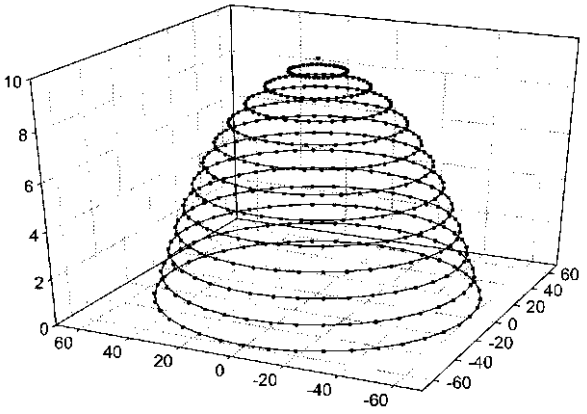

Fig. 8-12 *Uniform chromatic Riemannian plane constructed from segments between lines* m *and* o *in Fig. 8–11.*

hue difference, from metric chroma 10 to 100 approximately by a factor 4.6 rather than the factor 10 implicit in the euclidean chromatic diagram. The S_H factor should be verified with direct hue difference judgments.

There are two important conclusions to be drawn from this result:

1. Constant hue angle difference between colors of two hues does not imply constant perceived hue difference.
2. As a consequence a color space based on S_H cannot be euclidean because uniform slices created by S_H do not add up to form a flat circular plane. When forming a complete hue/chroma plane from segments between lines *m* and *o* of Fig. 8-11, a Riemannian plane (Fig. 8-12) is obtained.

8.7 UNIT DIFFERENCE CONTOURS AROUND THE HUE CIRCLE

Hue Angle versus Ellipse Angle

Color difference formulas derived from CIELAB imply that (with exception of colors of near unique blue hue) colors of constant hue lie on radial lines in the a^*, b^* diagram. While this is reasonably well the case for constant hue lines of the Munsell system, it is less so for those of NCS. As a first approximation we can assume, however, that this rule applies. The question arises if the conjecture that hue and chroma difference perception mechanisms shape unit difference contours of color difference data is well supported by data at the small color difference level. To assess this matter, 139 ellipses fitted to L-R (Melgosa et al., 1994) as well as R-D data (Melgosa et al., 1997) were investigated (11 with metric chroma <5 were excluded). The correlation coefficient between the CIELAB hue angle of the center color and the ellipse angle Θ

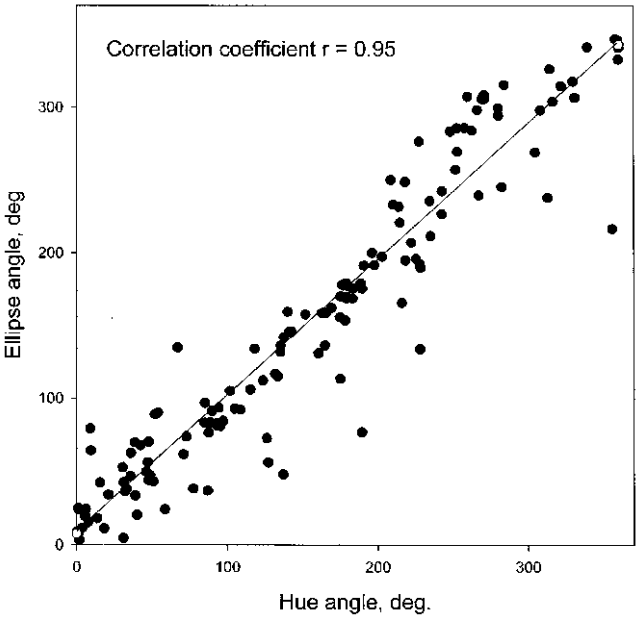

Fig. 8-13 *Scatter diagram of angle of major ellipse axis (ellipse angle) versus hue angle for the combined set of Luo and Rigg and RIT-DuPont ellipses with linear regression line.*

was calculated as 0.95. As the scatter diagram of Fig. 8-13 indicates, significant discrepancies appear to be random. When investigating the R-D data separately (n = 16), the correlation coefficient is found to be 0.88. After deleting two outliers that indicate longer axes in the hue direction than the chroma direction, the correlation coefficient increases to 0.98. Angles of the 11 near-neutral ellipses for the complete data set are found to range from 53 to 136.

While it is evident that CIELAB is not a good basis model for a uniform chromatic diagram and there is the fact that transformation of ellipses fitted in the CIE chromaticity diagram into ellipses in a^*, b^* involves a certain amount of error (Melgosa et al., 1994), the surprisingly high correlation coefficient appears to provide solid support for the conjecture of unit contours being aligned with constant hue lines. The conjecture is found to apply also to unit contours in the Munsell system and, as seen in Chapter 7, in OSA-UCS. A tendency in this direction was also found in quadrant 4 of the Wyszecki-Fielder color-matching error data. The alignment of fitted small color difference contours in the chromatic diagram has resulted in color difference calculation being performed in a polar coordinate rather than a rectangular system.

Additional data have in recent years been provided by J. Krauskopf and K. R. Gegenfurtner (K-G, 1992) and by M. J. Sankeralli and K. T. Mullen (1999). K-G determined visual thresholds around sixteen colors placed equidistant

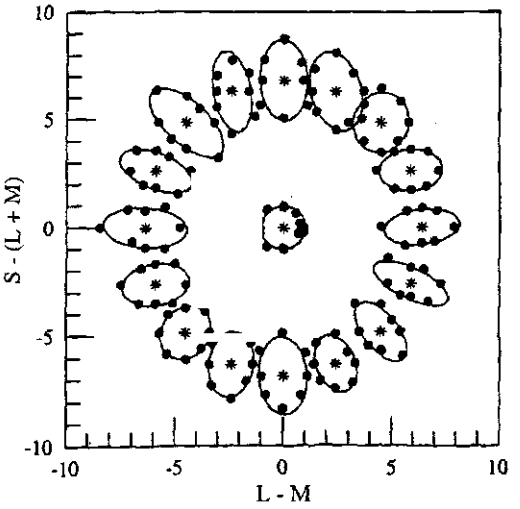

Fig. 8-14 *Visual thresholds around sixteen colors placed equidistant from the white point in the center of the cone opponent diagram. From Krauskopf and Gegenfurtner (1992).*

from the white point in a cone threshold diagram (see Fig. 8-14). In this diagram the scales of the two axes have been adjusted so that a circular contour is formed by the thresholds surrounding the white point. Most of the resulting fitted threshold contours are ellipses more or less pointing toward the achromatic point of the diagram. The fact that they do not closely do so in all cases is an aspect of the controversy concerning the number of hue detection mechanisms in the human visual system (as briefly discussed in Chapter 5). Sankeralli and Mullen (1999) determined unit chromatic contours at the 45° and 135° angles of a normalized cone based diagram with the axes $L - M$ and $S - (L + M)/2$ in the observer's personal isoluminant plane. The more or less elliptical contours are aligned well with the corresponding hue angles.

Ellipse Shape, Size, and Relation to Hue Angle, Metric Chroma, and Metric Lightness

In Chapter 7 it was shown that the ratio of contour axis length for the Munsell colors at moderate chroma has been determined as approximately 2:1 (2.8:1 at JND level). On average, a ratio of about 2:1 applies to the OSA-UCS data (see Section 7.2). Based on a regression of axis length versus metric chroma of the combined Luo and Rigg and RIT-DuPont set, the average major and minor axis lengths are found to be $a = 1.7$, $b = 0.80$ at $C^* = 0$ and $a = 4.1$ and $b = 1.92$ at $C^* = 100$ (ratio of 2.14:1). For seven near-neutral colors the ratio is found to be 1.55:1. The value of 2.14:1 is less than that found by Bellamy and Newhall. The average ratio of the Krauskopf and Gegenfurtner contours is found to be 1.7:1. The values for the Sankeralli and Mullen contours differ

TABLE 8-5 Correlation coefficients for the relationship between ellipse area and metric lightness *L, Luo and Rigg and RIT-DuPont data**

Metric Chroma C*	Correlation Coefficient	Number of Samples
10–20	0.06	21
20–30	–0.19	25
30–40	–0.64	27
31.00–34.99	–0.63	15
40–50	–0.10	21
60–70	0.19	11

I calculated these rusults from the L–R and R–D data.

by observer, with a ratio of 2.4:1 for one and 1.9:1 for the other. Undoubtedly, the experimental conditions also affect the ratio.

When determining the relationship between the length of the major axis and metric chroma for the L-R and R-D data, a correlation coefficient of 0.77 is found ($n = 150$), indicating good correlation. An only slightly lower value is found when comparing ellipse area against metric chroma (0.74). This level of correlation is another expression of the activity of the chromatic crispening effect. On the other hand, no correlation was found when comparing ellipse area and hue angle. In the limited metric chroma range of $C^* = 30 - 40$ ($n = 27$) the correlation coefficient is –0.01.

An unexpected result was obtained when comparing ellipse area against metric lightness L^* as a function of metric chroma. The results are found in Table 8-5. They indicate a considerable negative correlation between lightness and ellipse area for metric chroma values between approximately 25 and 45. That is, in this chroma range the ellipses become smaller as lightness increases. Based on the regression the average ellipse area in the metric chroma range of 30 to 40 is 18.1 at metric lightness 20 and 8.7 at metric lightness 80, a ratio of approximately 2:1. It is not evident what the cause of this finding is, and it requires further investigation and formula fitting.

As discussed in Chapter 4, there is little doubt that lightness and hue are fundamental color attributes. Chroma (contrast) is the necessary third attribute to represent all possible object colors systematically. Regardless of the mechanism we assume for the generation of hue (two process or multiprocess) it seems to be a matter of fact that in terms of a psychophysical presentation, we are more sensitive to stimulus increments if they signal hue changes than if they signal chroma changes. In a psychological or psychophysical diagram the outcome is an elongated unit contour. In practical terms, there appear to be two independent systems: one that assesses changes in the ratio of two opponent color signals (assuming a two-process hue detection system) and the other changes in the size of the vector sum of the opponent color system (indicative of contrast). Both are affected by surround. The two seemingly operate independently of each other and are not connected in a euclidean sense. A euclidean space can only be achieved (and only for

small color differences) with the help of euclidization operations such as the one by Thomsen.

In Chapter 5 we observed that there are different numbers of constant size hue differences between unique hues. As a result, in a chromatic diagram in which constant hue differences occupy equal hue angles (e.g., the Munsell system), unique hues do not fall on the diagram axes. On the other hand, in a diagram where the unique hues fall on the axes, equal hue angle differences do not indicate equal hue differences. To understand this situation, we require knowledge of the mechanism resulting in unique hues and of the hue difference mechanism.

8.8 GLOBAL DIFFERENCES

Differences of the Munsell or OSA-UCS step size are not the largest differences that can be compared in a color space. It is possible to think of more global kinds of differences by posing questions like:

1. Are the hue differences between the four unique hues the same?
2. Are the differences between colors falling on axes (however chosen) in the Munsell psychological diagram and the central gray of the same magnitude, and is gray in fact exactly in the middle between such colors?

The first question has already been answered in terms of the varying number of hue differences between the unique hues. Questions of the second kind were of interest to Judd and discussed by him in his article *Ideal color space* (1969). Based on his experiments with Munsell chips, he concluded that the superimportance of hue gradually fades as hue differences become very large.

Of Judd's observers a majority decided that the shortest path between opposing axis colors was not through gray but through a desaturated, hued color halfway between the opposing colors being compared. Judd worked out a function that accomplishes this fade for the modified Godlove difference formula (equation 4-2). But he indicated that there appears to be no geometrical model corresponding to his formulation, "at least, I have not been able to think of one." He concluded that also from this viewpoint ideal color space was impossible. Additional complications appear to arise when considering very large color differences.

8.9 HOW FUNDAMENTAL ARE THE VARIOUS KINDS OF DATA?

A goal of vision science is to uncover fundamental color vision processes. For this reason experimental conditions tend to be rigorously controlled to expose only one assumed process at a time to experimental variability. Exposures to

test stimuli tend to be very short to minimize changes in adaptation due to the test stimulus.

Color-scaling experiments, on the other hand, usually involve unlimited exposure times. Experimental conditions usually varied between different experiments and the degree of adaptation (in experiments involving small or large suprathreshold experiments) were not considered nor decisively controlled. As a result it is unlikely that fundamental processes have been determined but rather that the results represent overlapping fundamental processes (if it is possible to identify fundamental processes in this manner), however, often representative of practice in visual color quality control and of more natural viewing conditions.

In natural viewing conditions adaptation tends to change continuously as a result of what is being viewed, and the observer controls exposure times. If I harvest ripe strawberries in a strawberry patch, as I change my gaze, the visual system is adapted in various degrees to, among other things, combinations of the brownish-grayish color of soil, the green leaves of the strawberry plants, and, if there are plenty of ripe strawberries, the redness of the fruit. It is known that some adaptation processes proceed very rapidly in time while others are slower. Perceived color differences between two adjoining strawberries are a result of the total momentary adaptation situation.

It remains to be seen how large the differences are between the two kinds of observation conditions. In addition the observer groups in different experiments most always are different. Variations in the results of different observers are well known. They can be due to variations in their cone response functions or other components of their color vision system. The degree of linear transformability of individual color-matching functions remains to be determined as well if meaningful transformable means can be calculated from individual results. As discussed earlier, there is the possibility that certain judgments may be influenced by evolutionary experiences.

It is important to keep in mind that the following conclusions are valid only for a general viewing condition where the surround is achromatic and in luminance/lightness somewhere between the upper and lower extremes of the targets used in testing. At the color-matching error level we have found variation among observers and, possibly, experimental conditions. The MacAdam data are well represented by elongated rectangles in the L, S diagram. Both Wyszecki-Fielder observers here investigated (GW and AR) produced ellipses pointing already to some degree in the direction of the neutral point, most strongly so in the fourth quadrant (this applies also to the third observer). The impression is created that under the conditions of the MacAdam experiment, or at least for that observer, CME is not influenced by specific properties of the opponent color system but is based only on cone response limitations. Under the conditions of the Wyszecki-Fielder CME experiment, rotation of unit ellipses in the direction of the neutral point begins to be noticeable particularly in one quadrant. The same applies to the color difference matching results. At the level of thresholds the opponent color

system appears fully engaged (change in X to Z ratio, general alignment of unit contours in the direction of the neutral point) and remains so through large color differences.

It is not obvious what the cause of the rotation of a specific portion of the contours in the Wyszecki-Fielder CME and CDM data is. The MacAdam and Brown-MacAdam experiments employed monocular viewing. In both cases the surround was neutral. In the case of the MacAdam experiment, it was at half the luminance of the test fields; in case of Brown-MacAdam, it was dark. Ellipse rotation toward the neutral point is also noticeable in the five most highly saturated yellowish red colors of observer WRJB. In the Brown experiment a binocular colorimeter was used with a neutral surround slightly less luminous than the least luminous of the test fields. Ellipse rotation here is evident for the two most highly saturated yellowish red colors. The Wyszecki-Fielder CME experiments used two fields of a seven-field binocular colorimeter. The neutral surround was at half the luminance of the test field. As is mentioned in Wyszecki-Stiles, ". . . both eyes . . . could wander over the field with no strict fixation. . . . These conditions . . . approximated most closely those of ordinary viewing." The surrounds in all cases were large compared to the test fields. As mentioned, ellipse rotation is evident in the yellow-to-red segment for all three observers.

Data analysis in this chapter has been pursued based on a conventional view of color vision. From the results we can draw a number of conclusions regarding the various divisions of a common psychophysical color space (e.g., CIELAB), based on the magnitude of differences involved. Before going into details it should be mentioned again that the experimental basis at the various levels tends to be different. Color-matching errors and thresholds are usually determined using visual colorimeters. Small suprathreshold, medium, and large differences have usually been determined using color samples of some kind viewed in varied surroundings or, more frequently, in a light booth, usually in an achromatic surround.

The results of observer PGN in the MacAdam experiment indicate that hue discrimination was not explicitly active but that they are strictly a result of the sensitivity limitations of the three cone types. For both observers, in the Wyszecki-Fielder experiment, hue discrimination appears partially engaged (a number of ellipses point to the origin), but not all other aspects of the opponent color system (the average ratio between L and S increments is the same as in the MacAdam experiment and twice as large as in the Luo-Rigg and large color difference data). This implies engagement of different aspects of the system under different conditions. Lightness and chromatic crispening effects are engaged for CME data.

Based on the Richter data, at the threshold level all identified components are active. Suprathreshold small color difference unit ellipses, as we have seen, have a quite strong tendency to point to the origin. This effect is geometrically enhanced in the X, Z diagram, and even more if the X axis scaling is expanded

by a factor 2.3 for numerical balance with Z. Power modulation, lightness, and chromatic crispening apply at this level. The L or X increments have doubled compared to CME data, indicating increments in L or X that are not guided by cone sensitivity but by another mechanism, an opponent color system.

In differences of Munsell and OSA-UCS magnitude the opponent color system and hue discrimination are active, explicitly so in case of Munsell and implicitly in case of OSA-UCS, as we have seen. Lightness crispening is active as seen in the pre-1943 Munsell data and as recognized by inclusion of the effect in OSA-UCS. Chromatic crispening, however, has now faded. The result indicates that the processes guiding uniform tiling of color space are different at different levels of size of differences.